Water recovery via solar evaporation systems coupled to lithium mining from brines

Celso F. Baspineiro[1], Judith Franco[2] and Victoria Flexer[1]

1 Centro de Investigación y Desarrollo enMateriales Avanzados y Almacenamiento de Energía de Jujuy (CONICET-Universidad Nacional de Jujuy), Jujuy, Argentina

2 Instituto de investigaciones en energía no convencional (CONICET-Universidad Nacional de Salta), Salta, Argentina

Abstract

Extraction of lithium from continental brines is becoming a focus of importance worldwide. This is a vital raw material for the fabrication of lithium-ion batteries. The continued availability of lithium salts can only rely on a strong increase of mining and ore processing. Currently slightly more than half of the world production of lithium salts is extracted from brines, a practice that evaporates on average half a million litres of water per ton of lithium carbonate in highly desertic regions with intense solar irradiation and fresh water scarcity.

Taking into account the sustainability of the overall process with particular emphasis to water usage in relation to mining processes, we observe a potential link between lithium extraction from brines and desalination technologies. We consider here the possibility of recovering fresh water either in the current extractive process or with new extractive technologies, achieving a double objective: production of pure lithium salts and desalinated water.

There are several reported desalination technologies, and considering the high salinity of lithium rich brines, on average 300 g L-1 TDS, it is necessary to determine which of the already existing desalination technologies could be efficiently merged or coupled with lithium extraction in technical and economic terms. According to type of energy used and the climatic conditions mentioned, it is logical to think first of thermal solar desalination methods.

In this work, an experimental and theoretical analysis of brine desalination in the Cauchari Salar, in northwest Argentina, the performance of a simple solar still was analysed. The evaporation rate of the brine in the solar still was compared with the natural evaporation rate from open surface brine. Thermodynamic calculations to assess the least work of separation for fresh water and residual salts complement the analysis.

Keywords: Lithium mining from brines, Desalination, Pitzer model, least work of separation, Solar Still

1. Introduction

Lithium is an essential metal for the fabrication of lithium-ion rechargeable batteries. A steady increase of 8–11% in annual demand for lithium is anticipated in coming years [1], driven mostly by the electric vehicle industry [2]. Nowadays lithium is recovered worldwide from both hard rock ores (mostly spodumene) and continental brines [3]. Although the current production is roughly shared by 50/50 from both sources, lithium reserves in brines are much richer[3] and it is expected that in coming years mining from brines will represent a larger share [4].

Continental brines are high ionic strength solutions, of at least 170 g L−1 total dissolved solids (TDS), and most often TDS values around 300 g L−1. Lithium is a minor component in brines, usually representing 0.2-1.5 % of TDS, with sodium chloride being the major component and K+, Mg2+, Ca2+, borates and sulphates being other minor components [4]. Lithium rich brines are mostly concentrated in a small and arid region of South America, often referred to as the Lithium Triangle [5]. This region extends between northwest Argentina, southwest Bolivia and northern Chile. Other deposits can also be found in China, and the USA.

The technology currently in use for lithium extraction from brines consists in concentrate the brine by solar/wind evaporation. Only when the brine has lost approximately 90 % of its original water content, lithium carbonate is recovered after addition of soda ash, and some other chemical steps in a treatment plant. This technology for

doi:10.18086/swc.2019.46.01 Available at http://proceedings.ises.org

lithium extraction is generally known as the evaporitic technology [4, 6]. It is a low cost/high margin process and is relatively low-impact if compared, for example, to traditional mining and processing of metals from hard rocks.

Nevertheless it is also an extremely slow process, strongly dependent on both general climate and particular weather conditions [6]. The efficiency of the process will also be strongly dependent on the composition of other ions which are present at low concentrations, and that do not spontaneously precipitate in the ponds before the concentrated brine is pumped to the fine recovery plant.[3, 7, 8]

Regarding the overall sustainability of the whole process the water usage and waste generation / disposal are the big questions. We will focus our attention on the use of water. Evaporated water volume from brine is indeed huge: on average half a million litters per ton of lithium carbonate obtained [4]. Considering that a small lithium mining facility produces on average 20,000 tons of lithium carbonate per year, the amounts of evaporated water are huge. Water for industrial use is obtained from wells drilled and extracted from freshwater reservoirs. This freshwater has been subject of controversy because this is the same water used by both local communities in arid remote lands with fresh water scarcity, in these areas, it is more cost-effective to build small-scale water supply systems than to transport water, sometimes over long distances [9, 10] .

In this context, we propose to analyses the use of water desalination as a technology complementary to the evaporitic technology for the joint recovery of lithium salts and fresh water from the original brine. Desalinated water is in fact an industrial product different from natural water sources [11], and in this case, the recovered desalinated water could be used for industrial purposes, human consumption, and even irrigation, avoiding the depletion of natural reservoirs of fresh groundwater.

We see that desalination technologies and the evaporitic technology for lithium recovery, share the purpose of separating the water, to concentrate the brine and crystalize salts. Starting from this common ground, we decided to analyses the potential implementation of known desalination systems to the lithium brine mining industry. The first, rather obvious observation is the extremely high salinity of continental brines, with total salt concentration on average 9 times higher than sea water, in addition to its complex composition, with many different ionic species. However, the large volumes of water that could potentially be recovered, in addition to the limitations of the evaporitic technology are strong driving forces to pursue this study.

The high salinity will imply an energy-intensive process, which will make the resulting desalinated water more costly than other freshwater sources. However, in remote areas, which often have natural water sources that are not well protected and that are often brackish, desalination technology can be the best solution to providing safe drinking water [12]. The production cost should be analyzed in conjunction with the potential accelerated production of lithium salts.

Due to its geographical location and the high altitude, the Lithium Triangle area is one of the regions with the highest annual average global irradiation levels [13]. Moreover, solar-powered desalination systems are considered the most promising and most used renewable energy desalination technology. Coupling desalination systems with renewable energy sources represents an attractive solution for remote areas. In fact, around 70% of renewable energy desalination systems worldwide are solar-driven [14]. However, solar-powered desalination systems are currently not a common technology, representing only 0.02% of the total installed desalination capacity [15].

Solar-powered desalination systems can be classified as direct and indirect. Direct desalination systems are those that use solar energy directly without needing energy conversion, such as solar stills and solar humidification dehumidification systems. Considering the high salinity of the brine and the possibility of coupling the solar desalination technology in the lithium extraction process, direct desalination systems can tolerate feed water of any quality using low-grade energy with low operation and maintenance cost and are therefore suitable for decentralized systems.

2. Brine characteristics

Lithium-rich brine compositions are variable if different wells in the same salar are considered, and also temporal variability has been registered in the same well 10. There is quite a large variability in the range of concentrations reported for different brines, which is to be expected from the natural variability in brine composition [6, 16, 17]. We have applied our analysis to Cauchari, a small salt lake located in northwest Argentina, in the province of Jujuy, very close to the Chilean border. Despite variabilities between reports, certain trends can be found when comparing different reported concentrations, such as an approximate ratio between cations or anions

concentrations. Here we have chosen to make our calculations based on concentrations reported by Mohr et al. [18]. These values are reported in Table I.

Cations and anions concentrations are normally reported individually, however, thermodynamic calculations, require neutral salts to be identified. We have decided to pair all SO42- to Na2SO4 (i.e. SO42- molality equals Na2SO4 molality), and all K+, Mg2+, Li+ and Ca2+ to Cl- (K+ molality equals KCl molality, etc.). The remaining Na+ concentration (total moles of Na+ minus 2 times moles SO42-) represents NaCl concentration. Because both B and HCO3- represent below 0.1 % of total ions their concentrations have been neglected for thermodynamic calculations. For mock sea water, Mistry et al. 23 considered that salts with molal concentrations below 1 % could be neglected, therefore, we believe that our approximation should not produce important errors.

Tab 1: Cauchari brine concentration as reported by Mohr et al.[18]

Li ppm	K ppm	Mg ppm	Ca ppm	Na ppm	SO_4^{2-} ppm	Cl^- ppm	B ppm	HCO_3^- ppm	TOTAL SALINITY / g L^{-1}	Density g/ L^{-1}
510	4200	1450	330	93300	15700	148600	1120	670	265.88	1216

3. Thermodynamic calculations for activity coefficients

At the heart of the process of lithium salts production is the chemical energy of separating water, the solvent, and dissolved salts. The Gibbs free energy of a mixture is G.

$$G \equiv \sum_i n_i \mu_i \quad \text{(eq. 1)}$$

where n_i and μ_i are, respectively, the number of moles and chemical potential of species i.

The chemical potential is defined as

$$\mu_i \equiv \mu_i^{\circ} + RTlna_i \quad \text{(eq. 2)}$$

where the superindex ° denotes the standard (or reference) state, R is the molar (universal) gas constant, T is the absolute temperature in Kelvin, and a_i is the activity of each species i in the solution. The chemical activity a_i is related to the change in energy of a component as its concentration changes. It can be expressed as the product of the activity coefficient γ_i, times the concentration of that species. Here we will only use molality as a concentration scale (m_i, moles of solute per kilogram of solution):

$$a_{m,i} = \gamma_{m,i} m_i \quad \text{(eq. 3)}$$

$$a_{x,i} = \gamma_{x,i} x_i \quad \text{(eq. 4)}$$

where $\gamma_{m,i}$ is the molal activity coefficient if the molal concentration scale is used; and $\gamma_{x,i}$ is rational activity coefficient, if the molar fraction scale is used.

In the ideal solution model, the rational activity coefficient and the molal activity are both equal to unity. Physically, in an ideal solution, the introduction of a solute causes little change in the average interaction potential between all species. The activity coefficient γ thus represents departures from ideal solution behavior, and is the point of departure to compute G for electrolyte solutions.

For water, the solvent, activity is defined as

$$a_0 = \gamma_{f,0} x_0 \quad \text{(eq. 5)}$$

where $\gamma_{f,0}$ is the fugacity coefficient of the solvent, and x_0 its molar fraction. And hence, the chemical potential is expressed as

$$\mu_0 \equiv \mu_0^{\circ} + RTlna_0 \quad \text{(eq. 6)}$$

For water, the solvent, deviations from ideality are often expressed as an osmotic coefficient ϕ.

For a strong electrolyte salt, $C_{v_+} A_{v_-}$ which fully dissociates,

$$C_{v_+} A_{v_-} \rightarrow v_+ C^{z+} + v_- A^{z-} \quad \text{(eq. 7)}$$

where v_+ and v_- are the stoichiometric coefficients, and $z_+$and $z_-$are the ions respective charges

Mean concentration and mean activity coefficients are often more convenient and practical to use. The mean stoichiometric coefficient (v), the mean molal activity coefficient $\left(\gamma_{m,\pm}^{v}\right)$, and the mean molal concentration $\left(m_{\pm}^{v}\right)$ are defined as.

$$v \equiv v_+ + v_- \quad \text{(eq. 8)}$$

$$\gamma_{m,\pm}^{v} \equiv \gamma_{m,+}^{v_+}\, \gamma_{m,-}^{v_-} \quad \text{(eq. 9)}$$

$$m_{\pm}^{v} \equiv m_{+}^{v_+} m_{-}^{v_-} \quad \text{(eq. 10)}$$

The ionic strength of a solution, I_m, is calculated as

$$I_m = \frac{1}{2}\sum_i m_i z_i^2 \quad \text{(eq. 11)}$$

where the summation is over all solutes.

In mixed electrolyte solutions, the solution ionic strength is a function of the molalities of all species present. Therefore, the ionic strength can be significantly greater than molality of each single electrolyte species [19].

In Pitzer's model with effective molality, an effective molality m_{eff} is defined for each salt present in solution as

$$m_{eff} = \frac{2I_m}{v_+ z_+^2 + v_- z_-^2} \quad \text{(eq. 12)}$$

This effective molality is used in order to more accurately evaluate the molal activity coefficient of a single salt in a mixed electrolyte solution. After calculation of all effective molality values, the activity coefficient for each salt is calculated using the classical equations from the original Pitzer model for single electrolytes [19-22], equation (13).

$$ln\gamma_{m,CA} = |z_C z_A| f^{\gamma} + m_{\text{eff}} \frac{2v_C v_A}{v} B_{CA}^{\gamma} + m_{\text{eff}}{}^2 \frac{2(v_C v_A)^{3/2}}{v} C_{CA}^{\gamma} \quad \text{(eq. 13)}$$

Also the classical equation from the same model is used for the calculation of the molal osmotic coefficient ϕ.

$$\phi - 1 = |z_C z_A| f^{\phi} + m_{\text{eff}} \frac{2v_C v_A}{v} B_{CA}^{\phi} + m_{\text{eff}}{}^2 \frac{2(v_C v_A)^{3/2}}{v} C_{CA}^{\phi} \quad \text{(eq. 14)}$$

where

$$f^{\phi} = -A_{\phi} \frac{\sqrt{I_m}}{1 + b\sqrt{I_m}} \quad \text{(eq. 15)}$$

$$f^{\gamma} = -A_{\phi} \left[\frac{\sqrt{I_m}}{1 + b\sqrt{I_m}} + \frac{2}{b} ln\left(1 + b\sqrt{I_m}\right) \right] \quad \text{(eq. 16)}$$

$$B_{CA}^{\phi} = \beta_0 + \sum_{k=1}^{2} \beta_k exp\left(-\alpha_k \sqrt{I_m}\right) \quad \text{(eq. 17)}$$

$$B_{CA}^{\gamma} = 2\beta_0 + \sum_{k=1}^{2} \frac{2B_k}{\alpha_k^2 I_m} \left[1 - exp\left(-\alpha_k \sqrt{I_m}\right)\left(1 + \alpha_k \sqrt{I_m} - 0.5\alpha_k^2 I_m\right)\right] \quad \text{(eq. 18)}$$

$$C_{CA}^{\gamma} = \frac{3}{2} C_{CA}^{\phi} \quad \text{(eq. 19)}$$

$$b = 1.2 \quad \text{(eq. 20)}$$

Data for β_i,α_i, and C_{CA}^{ϕ} for a large collection of salt species are tabulated in the literature [20-22]. The constants α_2 and β_2 are only defined for 2:2 electrolytes, otherwise, set to zero.

The rational activity coefficient, $\gamma_{x,\pm}$ is easily obtained using

$$\gamma_{x,\pm} = \gamma_{m,\pm}(1 + M_0 \sum_s v_s m_s) \quad \text{(eq. 21)}$$

where the summation is over all electrolyte salts; m_s is the molality of each salt, and v_s is the number of moles of ions formed per mole of salt.

The molal activity of water, a_{H_2O} is written in terms of the molal osmotic coefficient

$$lna_{H_2O} = -vmM_{H_2O}\phi \quad \text{(eq. 22)}$$

The fugacity coefficient of water, γ_{f,H_2O} is evaluated using

$$ln\gamma_{f,H_2O} = -vmM_{H_2O}\phi - lnx_{H_2O} \quad \text{(eq. 23)}$$

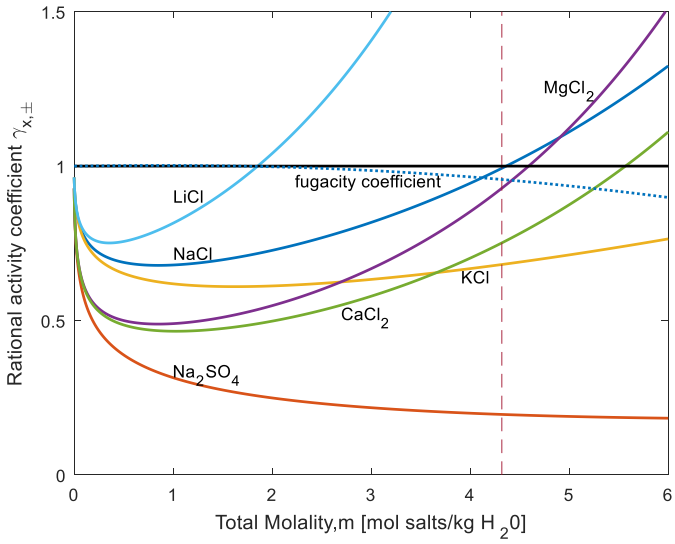

Fig 1: Rational activity and fugacity coefficients for all salts and the solvent (water) in Cauchari brine calculated using the Pitzer model with effective molality for mixed electrolytes.

Figure 1 shows the activity coefficients for all salts and the solvent fugacity coefficient in Cauchari brine calculated following equations (1) - (23). These coefficients are plotted vs total molality of the solution, in a solution where the ratio of concentrations between the different salts is maintained. The vertical line at total molality approximately 4.3, corresponds to Cauchari native brine (i.e. no processing). All values to the right of that vertical line correspond to coefficients from a brine that has being further concentrated, i.e. a brine that has lost water, either by solar/wind evaporation, or by some desalination system. All values to the left of the vertical line corresponds to concentrations of a hypothetical brine that is more diluted than a native brine, i.e. most likely those solutions would never be obtained in practice. However, those activity coefficients are It is important to note that for most salts the activity coefficients depart considerably from unity, i.e. their behaviour will depart considerably from that of ideal solutions. Interestingly, different salts show markedly different coefficients, compare for instance LiCl and NaCl.

These activity coefficients are the ones that are further used for the calculation of the saturation index and the least work of separation.

4. Saturation Indexes

Because of the high salinity, it is expected that precipitation of different salts will occur soon after the brine starts to get more concentrated (i.e. desalination begins). Table 2 shows solubility values for the different salts that could precipitate upon concentration of Cauchari brine. It is expected that a generic salt $M_M X_X$ will precipitate when QSP, defined according to (24), exceeds KSP, which is a tabulated value and is defined as (25) where the activities are those of a saturated solution.

$$Q_{SP} = a_M^{\nu_M} a_X^{\nu_X} \qquad \text{(eq. 24)}$$

$$K_{SP} = a_{M_{saturation}}^{\nu_M} a_{X_{saturation}}^{\nu_X} \qquad \text{(eq. 25)}$$

The saturation index, SI, is used for calculating whether a given salt in a solution is either super or sub saturated, i.e. whether thermodynamically it is expected that the salt will readily precipitate, or not. For SI > 0, the salt will precipitate. SI is defined as [23]:

$$SI = log\left(\frac{Q_{SP}}{K_{SP}}\right) \qquad \text{(eq. 26)}$$

It is expected that CaSO4 will precipitate right after desalination begins, since a very quick calculation shows that the QSP that can be estimated from concentration (not activity values) for this salt is about an order of magnitude higher than KSP, i.e. suggesting that the solution is either already saturated, or very close to saturation

in CaSO4. We consider pointless at this stage to make a precise calculation of saturation index based on activities for CaSO4. Although we expect CaSO4 to readily precipitate, at the most 1.12 g CaSO4 L-1 native brine will precipitate, since the Ca2+ concentration is quite small.

Water solubility values of all chlorides and all other sulphates are very high. The first salt that will precipitate should be NaCl, since despite its high solubility, the native brine already shows distinctly high concentrations of both Na+ and Cl- (see Table 1).

Tab 2: Solubility values in pure water (in g_{salt}/kg_{water}) Values taken from reference [24].

	NaCl	$MgCl_2$	KCl	LiCl	$CaCl_2$	Na_2SO_4	$CaSO_4$	$MgSO_4$	K_2SO_4	Li_2SO_4
Solubility g_{salt}/kg_{water}	360	560	355	845	813	281	2.05	357	120	342

In order to more accurately estimate at which concentration NaCl will start to precipitate, the SI for NaCl was calculated starting from the native brine concentration, and assuming that some desalination technology is concentrating the brine. Saturation indexes were calculated following Thiel and Lienhard [23]. The activity coefficients calculated according to (1) to (23) and shown in Figure 1 were used for the calculation of the SI. Figure 2 shows that up to 0.23 kg of pure water can be recovered from Cauchari brine before NaCl starts to precipitate.

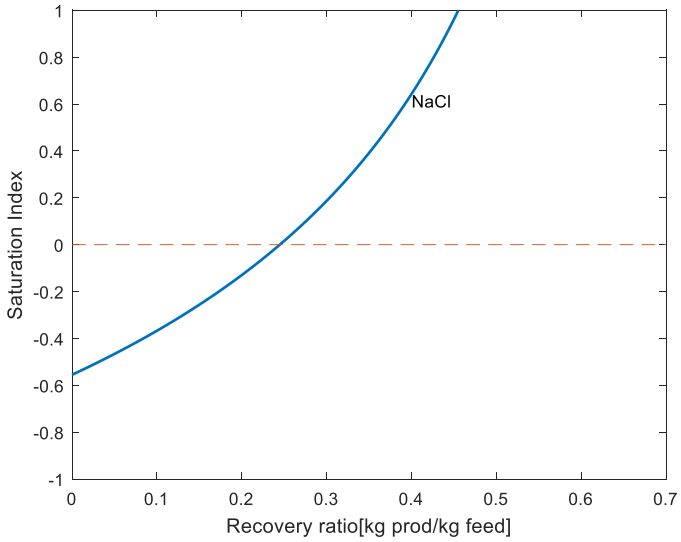

Fig 2: Saturation index for NaCl vs. water recovery ratio for Cauchari brine.

5. Calculation of least work of separation

The least work of separation, $\dot{W}_{least}$, defines the minimum amount of work required to separate a feed stream, into two streams of differing compositions, fresh water, and concentrated brine in the thermodynamic limit of reversible operation [19, 25]. The feed is denoted by $\boldsymbol{f}$; fresh water is noted $\boldsymbol{p}$, for product since in classical desalination systems the most important product is the fresh or desalinated water; and $\boldsymbol{b}$ is the notation for the concentrated brine. The reader should bear in mind that in classical desalination systems brine is the term used only for the product which is much more concentrated in salts than both the feed and the fresh water. However, all through this work we use the terms native brine for the feed solution, and concentrated brine, for the high salinity product. A derivation of the least work of separation in greater detail can be found in Mistry's work [19].

Combining the first and second laws of thermodynamics yields the rate of work separation.

$$\dot{W}_{sep} = \dot{G}_p + \dot{G}_b - \dot{G}_f + T_e \dot{S}_{gen} \qquad \text{(eq. 27)}$$

Where $\dot{G}_i$ is the flow rate of Gibbs free energy of stream i and $\dot{S}_{gen}$ is the total entropy generation resulting from the separation process. In the limit of reversible operation, entropy generation is zero and Eq. (27) reduces to the

least work of separation.

$$\dot{W}_{\text{least}} \equiv \dot{W}_{\text{sep}}^{\text{rev}} = \dot{G}_p + \dot{G}_b - \dot{G}_f \quad \text{(eq. 28)}$$

On a mass flow rate basis Eq. (28) is best written as

$$\dot{W}_{\text{least}} = \dot{m}g_p + \dot{m}g_b - \dot{m}g_f \quad \text{(eq. 29)}$$

Where g_j is the specific Gibbs free energy per kilogram of solution.

The recovery ratio is defined as the ratio of the mass flow rate of product water to the mass flow rate of feed water.

$$r \equiv \frac{\dot{m}_p}{\dot{m}_f} \quad \text{(eq. 30)}$$

Applying conservation of mass, and provided the feed and product salinities (S_f, S_p) are known, the concentrated brine salinity (S_b) is evaluated following (31):

$$S_b = \frac{S_f}{1-r} - \frac{rS_p}{1-r} \quad \text{(eq. 31)}$$

Therefore

$$\frac{\dot{W}_{\text{least}}}{\dot{m}_p} = \left(g_p - g_b\right) - \frac{1}{r}\left(g_f - g_b\right) \quad \text{(eq. 32)}$$

The least work of separation is a function of temperature, feed salinity, product salinity, and recovery ratio.

According to the objectives of this work, it is more convenient to express eq. (28) on a mole basis. Mistry and Lienhard showed that the least work for an single electrolyte $NaCl$ solution is given by.

$$\frac{\dot{W}_{\text{least}}}{\dot{n}_{H_2O,p}RT} = \left(ln\frac{a_{H_2O,p}}{a_{H_2O.b}} + m_{NaCl,p}M_{H_2O}ln\frac{a_{NaCl,p}}{a_{NaCl,b}}\right) - \frac{1}{r}\left(ln\frac{a_{H_2O,f}}{a_{H_2O,b}} + m_{NaCl,f}M_{H_2O}ln\frac{a_{NaCl,f}}{a_{NaCl,b}}\right) \quad \text{(eq. 33)}$$

Where the molar recovery ratio ($\bar{r}$) is defined as:

$$\bar{r} \equiv \frac{\dot{n}_{H_2O,p}}{\dot{n}_{H_2O,f}} = \frac{\text{molar flow rate of water in product}}{molar\ flow\ rate\ in\ feed} \quad \text{(eq. 34)}$$

Equation (33) can be generalized for a mixed electrolyte solution Eq. (13) to (15) whit Eq. (3) and (17) , and taking into account that we consider the product water as distilled water, $m_{NaCl,p} = 0$, thus we get:

$$\frac{\dot{W}_{\text{least}}}{\dot{n}_{H_2O,p}RT} = \left(ln\frac{a_{H_2O,p}}{a_{H_2O.b}}\right) - \frac{1}{r}\left(ln\frac{a_{H_2O,f}}{a_{H_2O,b}} + \sum_s m_{sf}\, M_{H_2O}ln\frac{a_{s,f}}{a_{s,b}}\right) \quad \text{(eq. 35)}$$

Where s represents all salt species that form the electrolyte mixture recipe and the activities of the solutes and solvent are defined by Eqs. (4) and (5) respectively

Figure 3 plots the results of calculating the least work of separation for producing distilled water quality from Cauchari brine. We can observe that, as we start recovering distilled water, i.e. recovery ratio > 0, the brine to be desalinated becomes more and more concentrated, and hence the least work of separation increases with the recovery ratio. Figure 3 is a calculation of the least work of separation until 0.24, the recovery ratio for which we have calculated that NaCl will start to precipitate (see Figure 2). While CaSO4 precipitation will only be minor at the very beginning of the desalination process, NaCl represents 90.04 % of the total salts on a molar basis (89.25 % on a mass basis). Therefore, when the solution gets supersaturated in NaCl, its precipitation will be unavoidable and it will constantly occur as long as fresh water can still be recovered. This massive precipitation will necessarily impose design constrictions for any desalination system. Therefore, at this point we have decided to calculate the least work of separation only for recovery ratios were NaCl does not precipitate.

Figure 3 also shows that the least work of separation for Cauchari brine is much higher than for analogous systems with lower TDS values [19, 23], starting already at a value of 26 kJ / Kg product, and reaching 33.4 kJ / Kg product for a recovery ratio of 0.24.

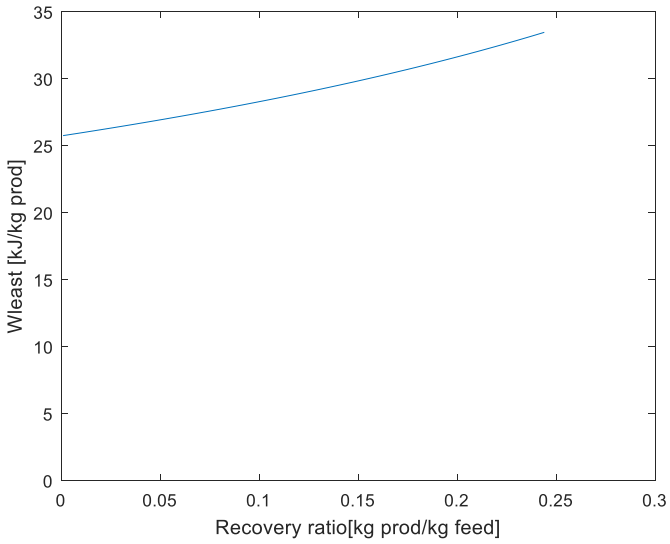

Fig 3: Least work of separation vs. water recovery ratio for Cauchari brine

6. The simplest desalination system: a solar still

We have observed in Figure 3 that the least work of separation, which is only a lower bound value for the specific work, is a relatively high value. Introducing any desalination technology into the lithium brine industry would imply entering into an economic competition with the current inexpensive solar/wind evaporitic technology, i.e. the operational cost of any desalination technology will be more costly than the current evaporitic technology. Therefore, from an economic point of view it will be difficult to convince private mining companies to increment both their OPEX and CAPEX to introduce any desalination technologies, despite the obvious advantage of potentially recovering large volumes of desalinated water as a by-product from the lithium mining industry, with potential positive environmental impact. In this unfavourable economic context, we have decided to test a simple solar desalination system as the easiest potential desalination system to implement in the lithium industry. Figure 4 shows figures of a simple solar still, built in house, which was installed at the edge of Cauchari salt lake (coordinates 23°34'47"S 66°43'52"W). The solar still capacity has a base of 2 m2, and it can contain brine up to a height of approximately 15 cm, although it is usually never filled beyond 10 cm (i.e. approximate capacity of 200 L). The picture in the right of figure 4 shows the concrete base that were adapted to help the solar still withstand the strong winds of the Puna plateau (on average of about 120 km h-1). Evaporated-condensed fresh water is recovered at the sides of the solar still and stored in the closed tank which is visible underneath the solar still in the front of the picture in photo of the left in Figure 4.

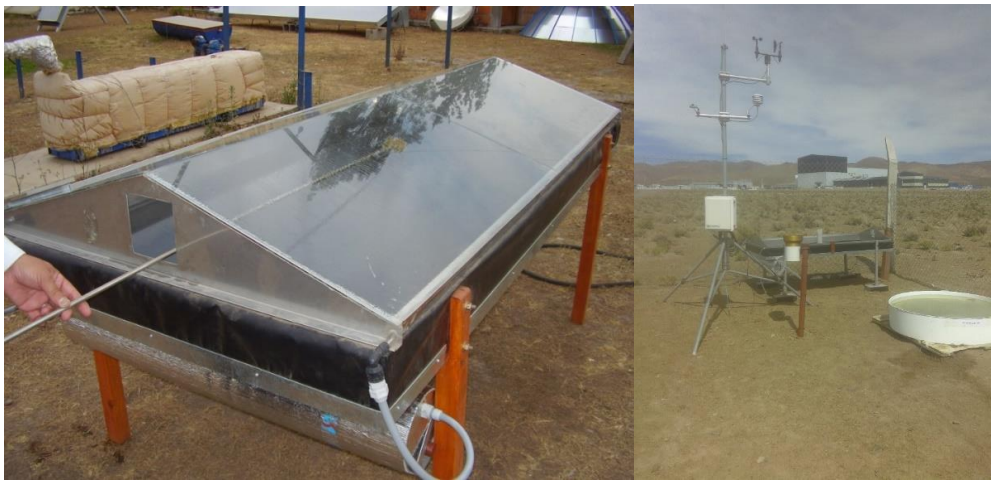

Fig 4: Simple solar still installed at the edge of Cauchari salt lake, in north western Argentina.

Next to the solar still, a small circular open pond was located (see photo to the right in figure 4). Both the solar

still and the solar pond were filled with native brine. The level of evaporated brine was measured on a daily basis in both the solar still and the open pond. In addition, the recovered fresh water was measured in the tank attached to the solar still. After the determination of the volume of evaporated water, both the solar still and the open pond were re-filled with exactly the same amount of tap water in order to restore the initial volume. Tap water was used in an attempt to keep the experiments with the same total salinity.

Figure 5 is a plot of the volume of water added to the solar still (red square dots) as a function of time, for a duration of approximately 5 months. The added water volume is compared to the volume of water recovered in the fresh water reservoir (blue circle dots). We can firstly observe that the evaporated water volume (which is equal to the added water volume) is consistently higher than the recovered water volume. These experimental data suggest that the despite our biggest effort to build up a tight and sealed solar still, some of the water vapour is escaping from the solar still before condensation, and therefore it is lost and not recovered. The amount of lost water vapour is about 60 % during the first month, while it decreases to about 20-30 % for the consecutive months.

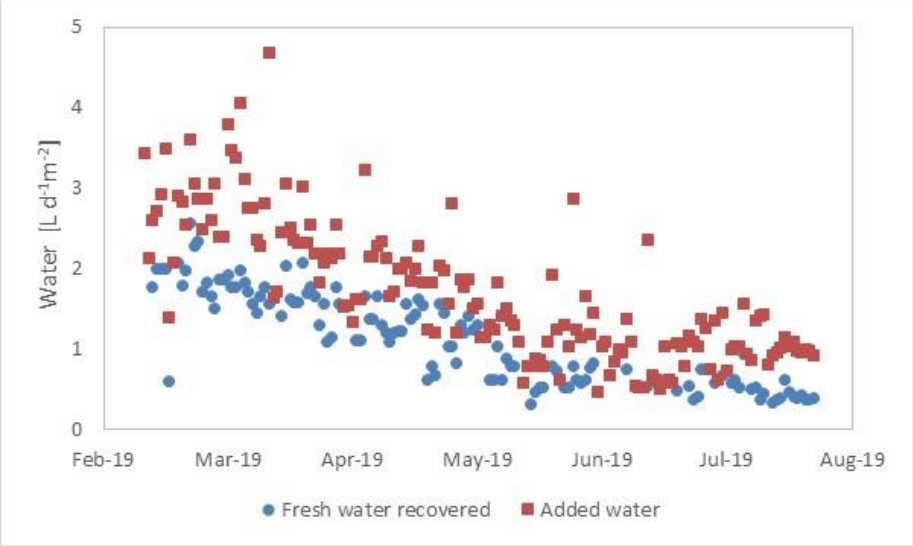

Fig 5: Added water vs recovered water - Solar Still

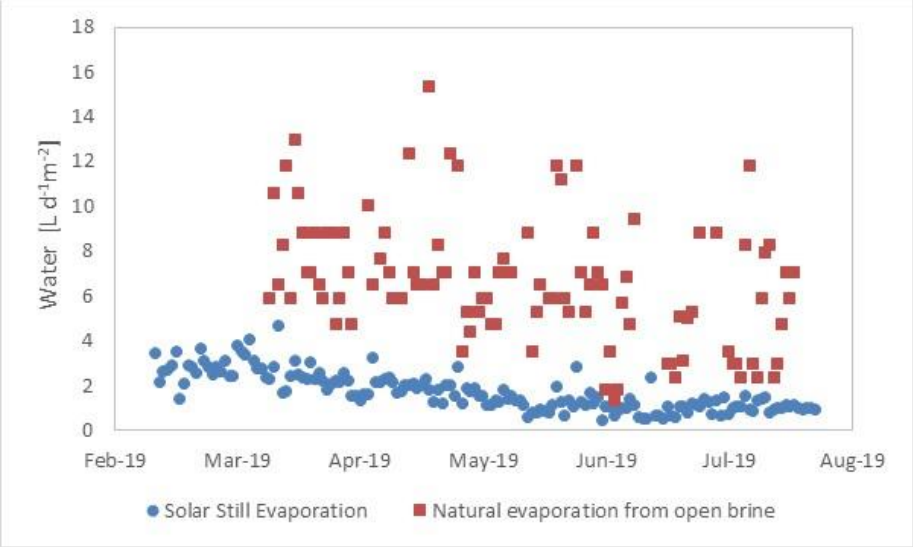

Fig 6: Solar Still evaporation vs Natural evaporation

This is probably due to the fact that silicone rubber was added on several occasions while running the experiment in order to try to minimize the said vapour losses. Some dispersion in the data points are also observed, which can be adscribed firstly to weather variations. The smallest graduation in the metric scale used to evaluate the amount of evaporated water was 1 mm only, which, for a base area of 2 m2 translates into a volume of 2 L, i.e. the reading error is considerable for the daily evaporated amount. Finally, a consistent trend can be observed both

the evaporated water volume and the recovered water volume. As the experiment advances, the water volumes decrease. This is attributed to seasonable variations in temperatures, indeed, the experiment was started at the end of the summer (February 2019), and it progressed into the autumn and winter months (Southern hemisphere).

Figure 6 is a plot of the water volume evaporated in the solar still (blue circle dots) and the water volume evaporated in the open pond (red square dots). Figure 6 shows that, on average the amount of water evaporated in the open pond is 3 times higher than in the solar still. It is known that in a open pond, the evaporation rate will be dependent on both brine temperature elevation (solar heating), and the constant removal of water vapour (wind blow) that makes the system depart from solution-vapour equilibrium. Conversely, the solar still seems to be affected quite differently by these variables. While in the closed system, the brine temperature will increase considerably, the cover of the solar still is blocking the removal of water vapour. The wind is acting indirectly only, via cooling down the solar still cover and facilitating water condensation. Data in figure 6 strongly suggest that in the open system the strong winds in the Puna plateau seem to have a much stronger effect on evaporation rate than heating. Figure 7 is a plot of the wind speed for the period of time considered, it shows a high average value with a random behaviour. A seasonality pattern is not observed but values are maintained around an average with some peaks.

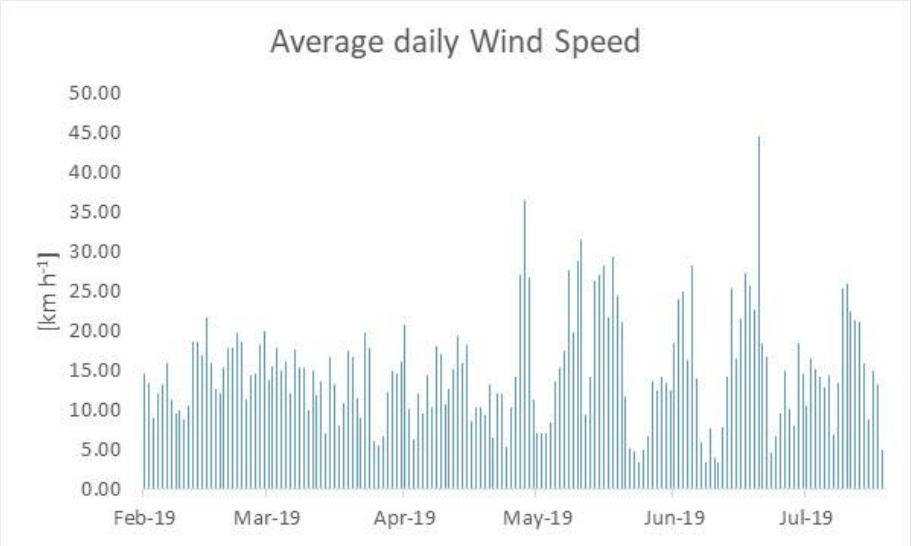

Fig 7: Average daily Wind Speed

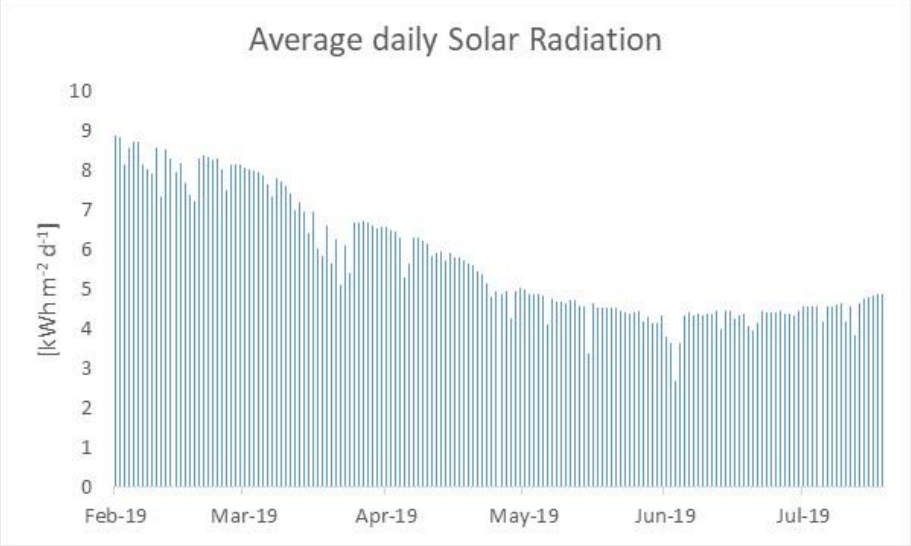

Fig 8: Average daily Solar Radiation

Figure 8 is a plot of the daily solar radiation for the period of time considered. It shows a seasonal decrease which directly affects the evaporation rate in Solar Still showing a similar behaviour.

7. Conclusions

In work presented here we have presented thermodynamic calculations to show the minimum work of separation for water recovery from a lithium-rich brine. Our idea is to couple known desalination technologies to lithium mining from brines. Our calculations have shown that the minimum work of separation is high and, as expected, increases with the recovery ratio. Therefore, only relatively inexpensive desalination systems have chances of being incorporated into the brine mining industry. We have constructed and tested a simple solar still as the easiest and most inexpensive solar desalination system that we believe could be implemented.

Our experimental results show that while water recovery values are encouraging to pursue research on this prospective technology, the incorporation of these solar stills would make water evaporation even slower than with current technology, open ponds. Our work in progress includes a detailed measuring of temperatures for all components of the solar still and we are attempting at modelling the heat exchanges. We are thinking in parallel about the possibility of constructing a humidification-dehumidification system that incorporates both the benefit of brine heating, wind convection and water recovery.

8. Acknowledgments

CFB acknowledges a doctoral fellowship from CONICET. VF and JF are permanent research fellows from CONICET. This project was funded by FITR-INDUSTRIA 9/2013 from ANPCyT.

9. References

1. Baylis, R. *Evaluating and forecasting the lithium market from a value perspective*. 2013. Las Vegas.
2. Opitz, A., et al., *Can Li-Ion batteries be the panacea for automotive applications?* Renewable and Sustainable Energy Reviews, 2017. **68**: p. 685-692.
3. Kesler, S.E., et al., *Global lithium resources: Relative importance of pegmatite, brine and other deposits.* Ore Geology Reviews, 2012. **48**: p. 55-69.
4. Flexer, V., C.F. Baspineiro, and C.I. Galli, *Lithium recovery from brines: A vital raw material for green energies with a potential environmental impact in its mining and processing.* Science of the Total Environment, 2018. **639**: p. 1188-1204.
5. Grosjean, C., et al., *Assessment of world lithium resources and consequences of their geographic distribution on the expected development of the electric vehicle industry.* Renewable and Sustainable Energy Reviews, 2012. **16**(3): p. 1735-1744.
6. Garrett, D.E., *Handbook of Lithium and Natural Calcium Chloride*, ed. E. Science. 2004.
7. Houston, J., et al., *The Evaluation of Brine Prospects and the Requirement for Modifications to Filing Standards.* Economic Geology, 2011. **106**(7): p. 1225-1239.
8. Choubey, P.K., et al., *Advance review on the exploitation of the prominent energy-storage element: Lithium. Part I: From mineral and brine resources.* Minerals Engineering, 2016. **89**: p. 119-137.
9. Peter-Varbanets, M., et al., *Decentralized systems for potable water and the potential of membrane technology.* Water Research, 2009. **43**(2): p. 245-265.
10. Glueckstern, P., *Design and operation of medium- and small-size desalination plants in remote areas: New perspective for improved reliability, durability and lower costs.* Desalination, 1999. **122**(2): p. 123-140.
11. Belessiotis, V., S. Kalogirou, and E. Delyannis, *Copyright*, in *Thermal Solar Desalination*. 2016, Academic Press. p. iv.
12. Kharraz, J.A., B.S. Richards, and A.I. Schäfer, *Chapter 3 - Autonomous Solar-Powered Desalination Systems for Remote Communities*, in *Desalination Sustainability*, H.A. Arafat, Editor. 2017, Elsevier. p. 75-125.
13. Pugsley, A., et al., *Global applicability of solar desalination.* Renewable Energy, 2016. **88**: p. 200-219.
14. Quteishat, K. and M. Abu-Arabi, *Promotion of Solar Desalination in the MENA Region*. 2018.

15. Delyannis, E. and V. Belessiotis. *A historical overview of renewable energies*. in *Proc. Mediterranean Conference on Renewable Energy Sources for Water Production, Santorini, Greece*. 1996.
16. *British Geological Service: Lithium*. 2016 [cited 2017 21st July]; Available from: https://www.bgs.ac.uk/mineralsuk/statistics/mineralProfiles.html.
17. Jaskula, B.W., *USGS: 2015 Minerals Yearbook: lithium [advanced released].* . 2017.
18. Mohr, S., G. Mudd, and Giurco, *Lithium Resources and Production: a critical global assessment*, in *Prepared for CSIRO Minerals Down Under Flagship, by the Institute for Sustainable Futures (University of Technology, Sydney) and Department of Civil Engineering (Monash University),*. 2010.
19. Mistry, K.H., H.A. Hunter, and J.H. Lienhard V, *Effect of composition and nonideal solution behavior on desalination calculations for mixed electrolyte solutions with comparison to seawater.* Desalination, 2013. **318**: p. 34-47.
20. Pitzer, K.S., *Thermodynamics of electrolytes. I. Theoretical basis and general equations.* The Journal of Physical Chemistry, 1973. **77**(2): p. 268-277.
21. Pitzer, K.S. and G. Mayorga, *Thermodynamics of electrolytes. II. Activity and osmotic coefficients for strong electrolytes with one or both ions univalent.* The Journal of Physical Chemistry, 1973. **77**(19): p. 2300-2308.
22. S. Pitzer, K. and G. Mayorga, *Thermodynamics of Electrolytes.: III. Activity and Osmotic Coefficients for 2–2 Electrolytes*. Vol. 3. 1974. 539-546.
23. Thiel, G.P. and J.H. Lienhard V, *Treating produced water from hydraulic fracturing: Composition effects on scale formation and desalination system selection.* Desalination, 2014. **346**: p. 54-69.
24. Lide, D.R., ed. *CRC Handbook of Chemistry and Physics 84th Edition*. 2003, CRC PRESS.
25. Mistry, K.H., et al., *Entropy Generation Analysis of Desalination Technologies.* Entropy, 2011. **13**(10): p. 1829.